

Characterizing a USP9X-COP1 regulatory axis of RIT1 protein abundance

Amanda Riley^{1,2}, Athea Vichas¹, Naomi T. Nkinsi¹, Phoebe C. R. Parrish^{1,3}, Shriya Kamlapurkar¹, and Alice H. Berger¹

¹ Human Biology Division, Fred Hutchinson Cancer Research Center, Seattle, WA

² Molecular and Cellular Biology Program, University of Washington, Seattle, WA

³ Department of Genome Sciences, University of Washington, Seattle, WA

University of Washington

Summary

Standard care of lung cancer is moving away from chemotherapy in favor of personalized approaches based on specific mutations in each tumor. Genome-sequencing studies have identified somatic mutations in the small GTPase *RIT1* (Ras-like in all tissues) in lung adenocarcinoma patients. Thousands of patients per year are diagnosed with *RIT1*-driven cancer, but treatment options are limited. A targeted therapy for *RIT1*-driven disease could greatly improve patient outcomes.

Little is known about how *RIT1* drives cellular transformation. To genetically dissect signaling pathways downstream of *RIT1*, we performed a genome-wide CRISPR/Cas9 screen in isogenic PC9 lung adenocarcinoma cells in which cell survival is dependent on expression of *RIT1*^{M90I}. In this system, *RIT1*-driven drug resistance provides a selectable phenotype to assess the growth effects of individual gene knockouts. Using this approach, we can identify genetic dependencies (genes that, when knocked out, confer a growth disadvantage) and cooperating factors (genes that, when knocked out, confer a growth advantage) in *RIT1*-mutant lung cancer cells. From this analysis, we identified the deubiquitinase *USP9X* and the E3 ubiquitin ligase *COP1* as genetic regulators of *RIT1* function. Previous work suggests that the protein abundance of *RIT1* is essential for its pathogenic function; given this, we propose a regulatory axis of *RIT1* protein abundance mediated by *USP9X* and *COP1*. I hypothesize that *USP9X* positively regulates *RIT1* protein levels while *COP1* counteracts this effect. This work is poised to not only expand our understanding of *RIT1* biology and oncogenic mechanisms, but it also identifies *USP9X* as a potential druggable target for the treatment of *RIT1*-driven cancers and other diseases characterized by *RIT1* mutations and amplifications.

RIT1 is mutated in lung adenocarcinoma

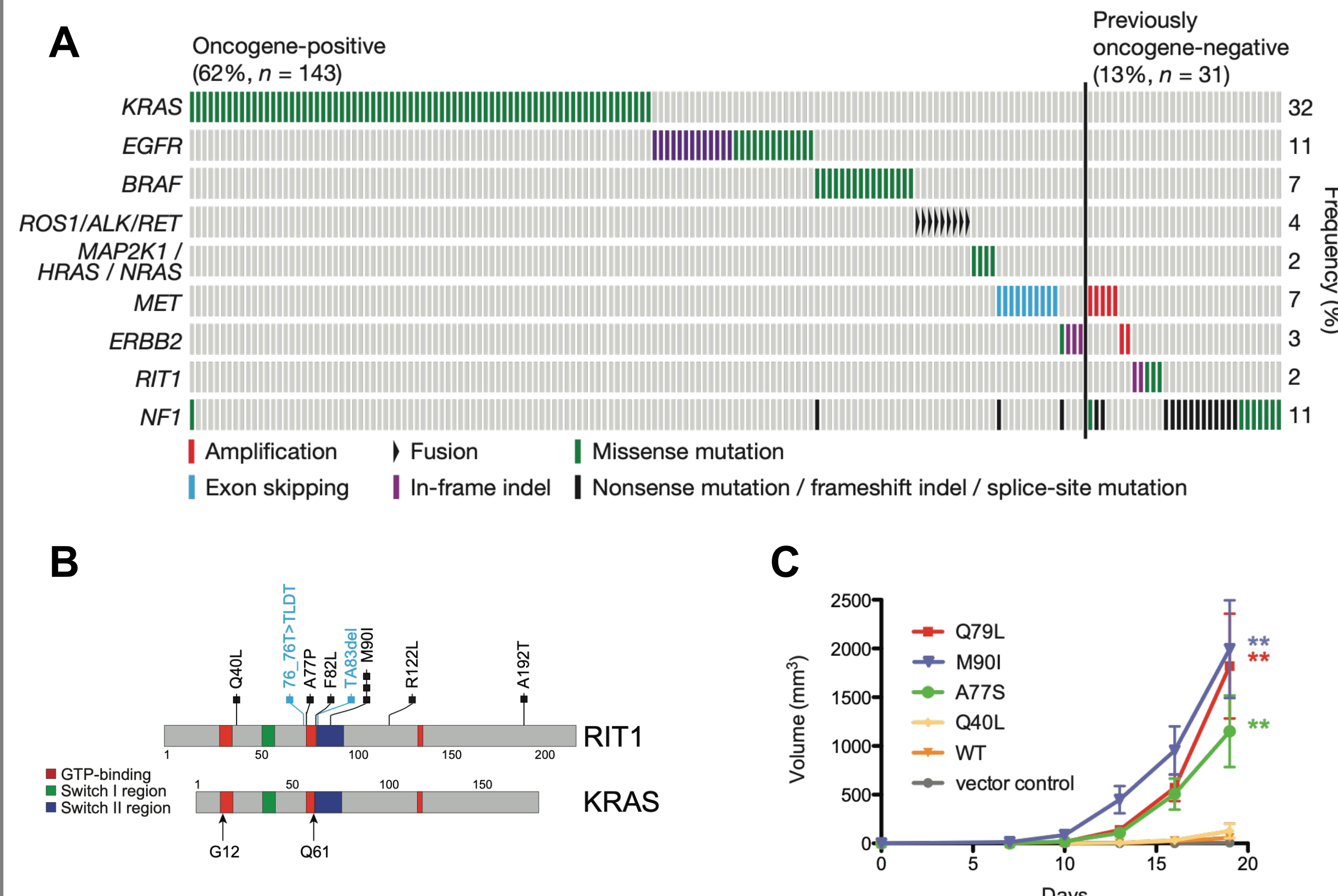


Figure 1. *RIT1* is oncogenic in lung adenocarcinoma.

A. Co-mutation plot depicting variants of known significance in the RTK/Ras/RAF pathway. *RIT1* mutations are mutually-exclusive with other known driver mutations in this pathway. (TCGA, 2014) **B.** *RIT1* is homologous in sequence and domains to *KRAS*. The 'hot spot' of transformative mutations in *RIT1* reside in the switch II domain of *RIT1*, including at amino acid 90. **C.** Tumor growth of xenografts of NIH3T3 cells. Data shown is mean \pm s.e.m. of nine replicates per construct. * $P < 0.01$ by two-tailed t-test. (Berger et al., 2014)

Assay system to identify genetic dependencies of *RIT1*-mutant cells

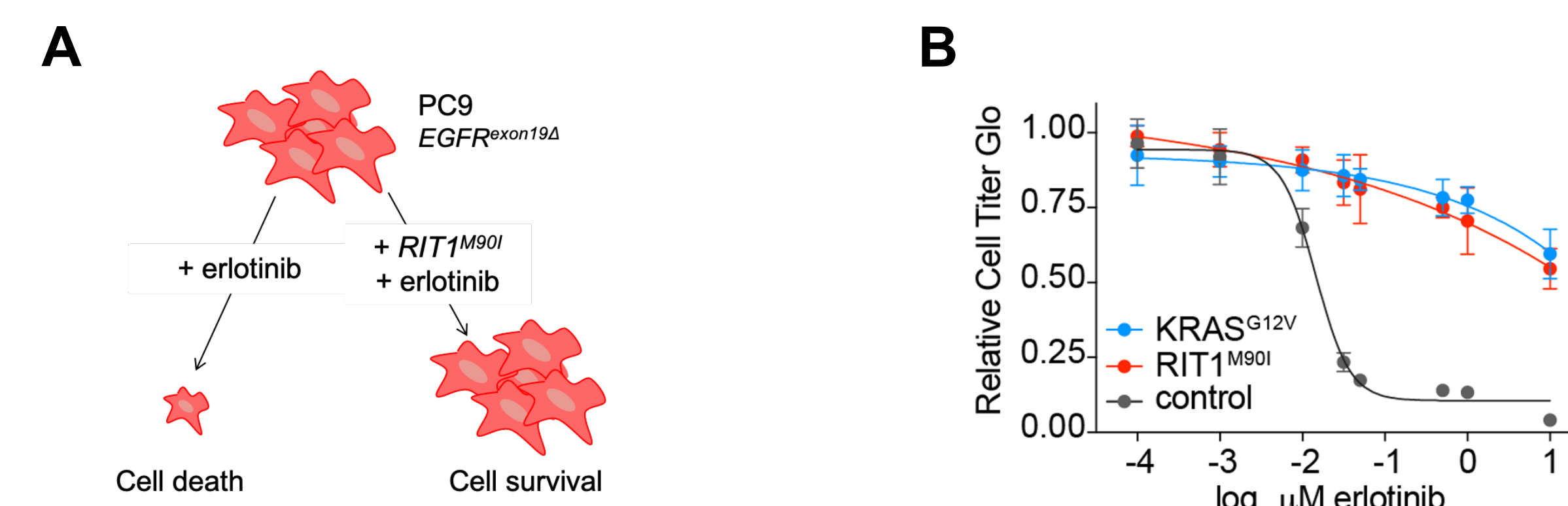


Figure 2. *RIT1*^{M90I} confers resistance to EGFR inhibition.

A. Schematic representation of erlotinib resistance in PC9 cells expressing *RIT1*^{M90I}. **B.** Dose-response of erlotinib in PC9-Cas9 parental cells (control) and PC9-Cas9 cells expressing *RIT1*^{M90I} or *KRAS*^{G12V}. Data shown is the mean and standard deviation of 8 technical replicates per cell line.

Genome-wide CRISPR/Cas9 screen in isogenic lung adenocarcinoma cell lines

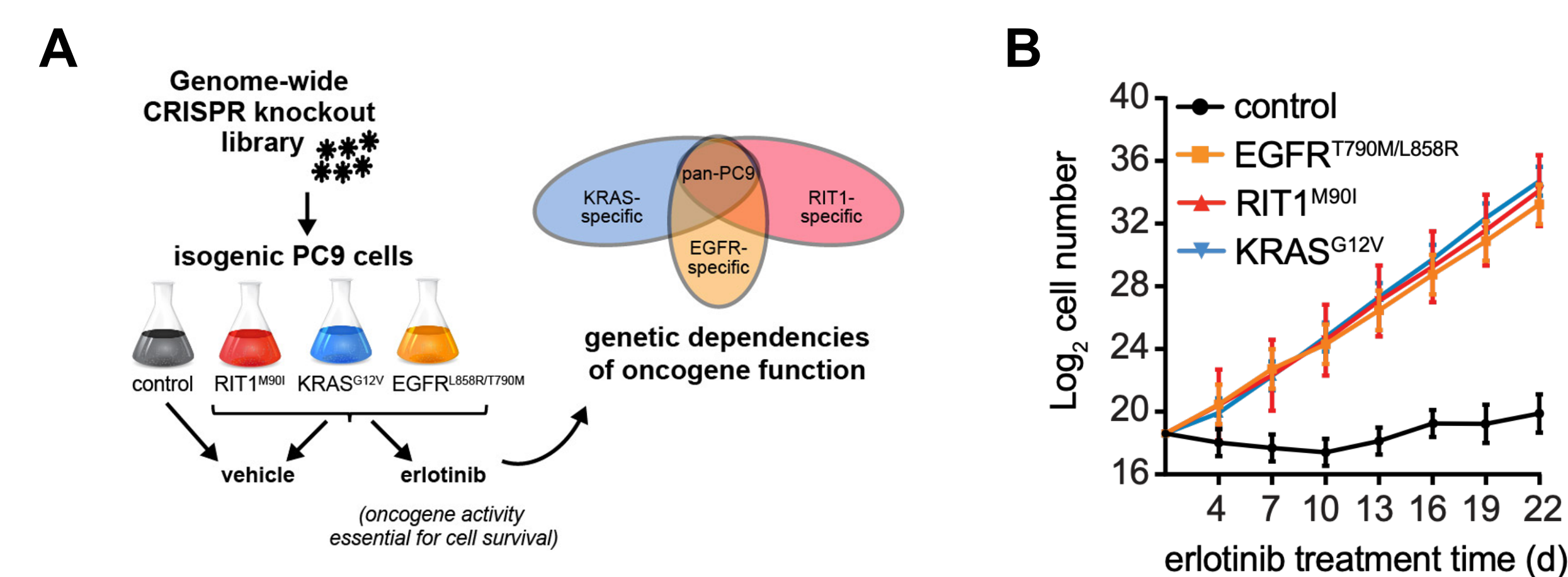


Figure 3. CRISPR/Cas9 screen in PC9-Cas9 cells expressing known oncogenes.

A. Schematic of CRISPR screens performed. Abundance of guide RNAs was compared between early time point and final (day 22 for DMSO and day 28 for erlotinib) time points. **B.** Proliferation assay of isogenic cell lines grown in 50nM erlotinib. Error bars indicate \pm 95% confidence interval of two replicates per cell line. All oncogene-expressing cell lines proliferate in erlotinib at a similar rate.

USP9X and *COP1* are key genetic players in *RIT1*-driven cell survival

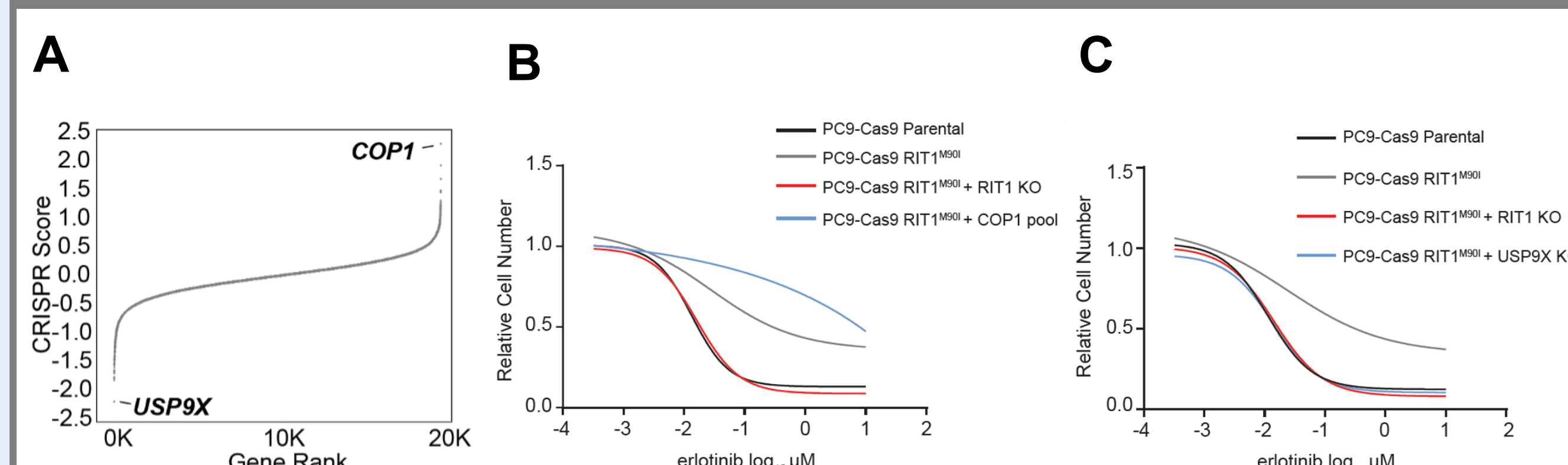


Figure 4. Identification of *USP9X* and *COP1* as *RIT1* regulators.

A. Rank plot of differential CRISPR score (normalized log₂(fold change) of the average of 4 sgRNAs per gene in two biological replicates) in PC9-Cas9-*RIT1*^{M90I} cells between erlotinib-treated and DMSO-treated screens. **B.** Dose response curve of control PC9 cells or pooled PC9-Cas9-*RIT1*^{M90I} cells with *RIT1* or *COP1* knockout (KO). **C.** Dose response curve of control PC9 cells or pooled PC9-Cas9-*RIT1*^{M90I} cells with *RIT1* or *USP9X* KO.

USP9X loss reduces *RIT1* protein abundance and stability

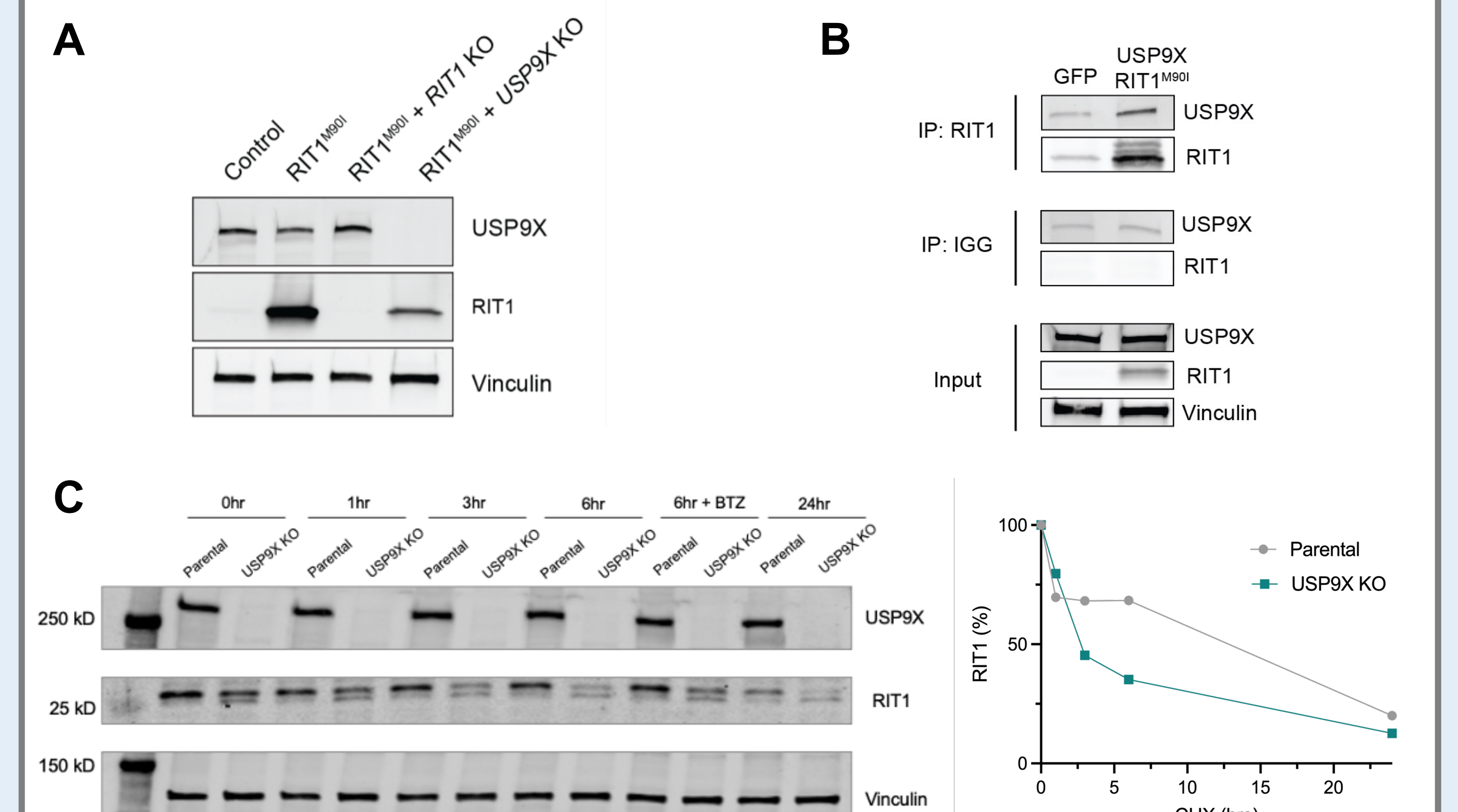


Figure 5. *USP9X* interacts with *RIT1* and regulates *RIT1* protein abundance.

A. Western blot of *RIT1* and *USP9X* in parental (control) PC9 cells or *RIT1* knockout (KO) and *USP9X* KO cells derived from PC9-Cas9-*RIT1*^{M90I}. Vinculin serves as loading control. **B.** Co-IP of *RIT1*^{M90I} and *USP9X* in HEK293T cells. Immunoprecipitation was performed with a control IGG antibody or *RIT1* antibody. Vinculin serves as a loading control. **C. left**, PC9-Cas9 parental and *USP9X* KO cells were treated with 20 μ g/mL cycloheximide (CHX) for indicated amounts of time. 100nM of the proteasome inhibitor bortezomib (+BTZ) was used to rescue degradation. Vinculin serves as a loading control. **right**, half-life of *RIT1* based on quantitative analysis of relative band intensity in western blot on left.

USP9X as a novel druggable target in *RIT1*-driven diseases

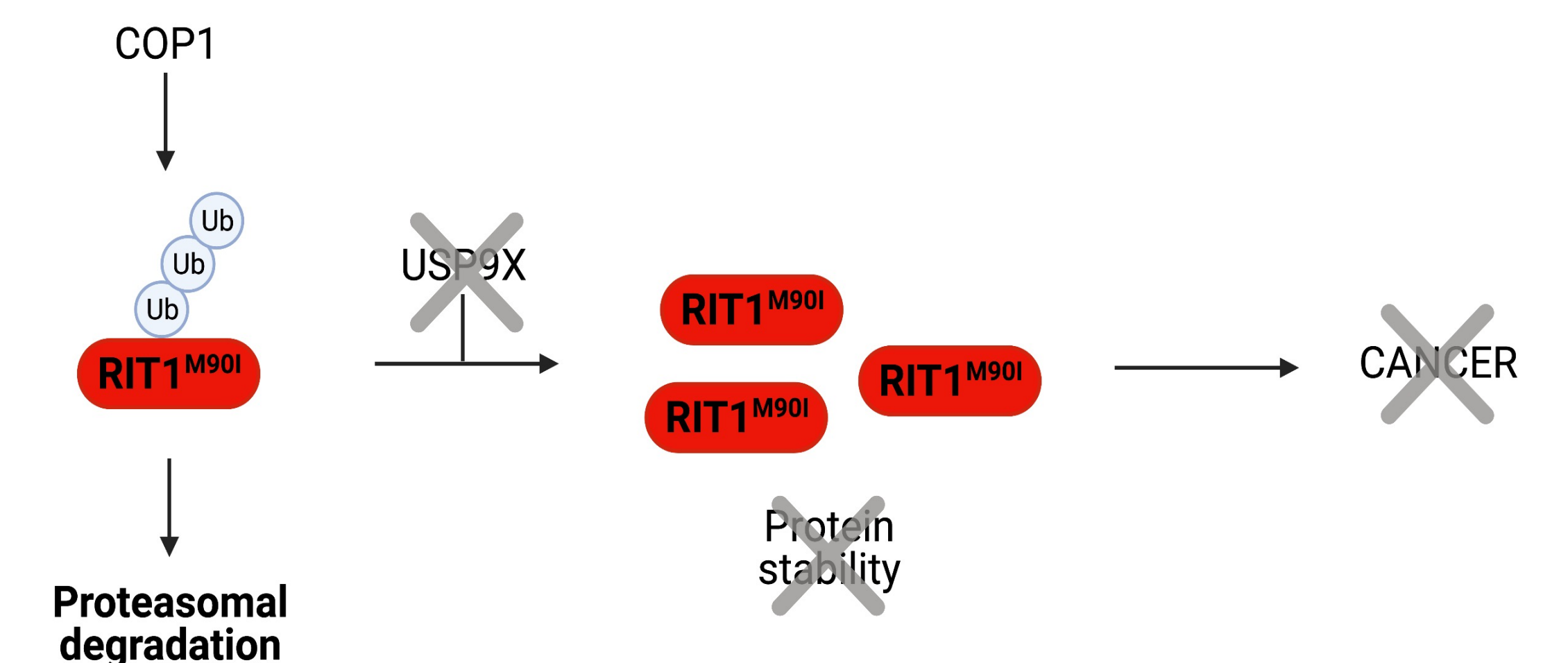


Figure 6. Proposed model of *USP9X* as a therapeutic vulnerability in *RIT1*-mutant cells. *USP9X* knockout or inhibition is predicted to reduce *RIT1* protein stability and abrogate *RIT1*-driven cancer.

References

Vichas, A., Riley A.K., Nkinsi, N.T., Kamlapurkar, S., Parrish, P.C.R., Lo, A., Duke, F., Chen, J., Fung, I., Watson, J., et al. (2021). Integrative oncogene-dependency mapping identifies *RIT1* vulnerabilities and synergies in lung cancer. *Nat. Commun.* 12, 4789. *equal contribution

Funding Sources

This research was funded in part through NCI grant R00CA197762 to A.H.B., donations from the Smith family to A.H.B., NIH/NCI Cancer Center Support Grant P30 CA015704 New Investigator support to A.H.B., a Lung Cancer Research Foundation Research Grant to A.V., the Hutch United postdoctoral fellowship to A.V. A.R. was supported in part by PHS NRSA T32GM007270 from NIGMS. P.C.R.P. was supported in part by NSF DGE-1762114.